Biophysical Journal
Article

Biophysical Society

Desmosomal Hyperadhesion Is Accompanied with Enhanced Binding Strength of Desmoglein 3 Molecules

Michael Fuchs,[1] Anna Magdalena Sigmund,[1] Jens Waschke,[1] and Franziska Vielmuth[1,*]
[1]Institute of Anatomy, Faculty of Medicine, Ludwig-Maximilians-Universität Munich, Munich, Germany

ABSTRACT Intercellular adhesion of keratinocytes depends critically on desmosomes that, during maturation, acquire a hyperadhesive and thus Ca^{2+} independent state. Here, we investigated the roles of desmoglein (Dsg) 3 and plakophilins (Pkps) in hyperadhesion. Atomic force microscopy single molecule force mappings revealed increased Dsg3 molecules but not Dsg1 molecules binding strength in murine keratinocytes. However, keratinocytes lacking Dsg3 or Pkp1 or 3 revealed reduced Ca^{2+} independency. In addition, Pkp1- or 3-deficient keratinocytes did not exhibit changes in Dsg3 binding on the molecular level. Further, wild-type keratinocytes showed increased levels of Dsg3 oligomers during acquisition of hyperadhesion, and Pkp1 deficiency abolished the formation of Ca^{2+} independent Dsg3 oligomers. In concordance, immunostaining for Dsg1 but not for Dsg3 was reduced after 24 h of Ca^{2+} chelation in an ex vivo human skin model, suggesting that desmosomal cadherins may have different roles during acquisition of hyperadhesion. Taken together, these data indicate that hyperadhesion may not be a state acquired by entire desmosomes but rather is paralleled by enhanced binding of specific Dsg isoforms such as Dsg3, a process for which plaque proteins including Pkp 1 and 3 are required as well.

SIGNIFICANCE Desmosomes provide adhesive strength to tissues constantly exposed to mechanical stress. They consist of different protein families, including desmosomal cadherins, which maintain strong interaction with their extracellular domains, and plaque proteins, among them plakophilins. Plakophilins are involved in desmosomal turnover and hyperadhesion, a state at which desmosomal cadherins become independent of extracellular Ca^{2+}. However, the molecular mechanisms underlying hyperadhesion are not yet fully elucidated. In this study, the authors show that hyperadhesion may not be a state acquired by entire desmosomes. The data indicate that it is rather paralleled by alterations of specific desmosomal cadherin binding properties, such as changes in clustering and single molecules binding strength. These changes also require the plaque proteins plakophilin 1 and 3.

INTRODUCTION

Tissues such as the myocardium or the epidermis experience constantly mechanical pressure and shear stress (1–3). Desmosomes are crucial to withstand this mechanical stress by the maintenance of strong intercellular adhesion. The importance of desmosomes is reflected by diseases targeting desmosomal proteins such as pemphigus, in which cell cohesion is impaired by autoantibodies against the desmosomal cadherins desmoglein (Dsg) 1 and 3 (4,5), or ectodermal dysplasia skin fragility syndrome caused by mutations affecting the desmosomal plaque protein plakophilin (Pkp) 1 (6,7). On a molecular level, desmosomes consist of desmosomal cadherins that maintain intercellular adhesion via their extracellular domains in a Ca^{2+} dependent, both homo- and heterophilic manner (8–10). Via the plaque proteins plakoglobin, Pkps, and desmoplakin, desmosomes are linked to the intermediate filament cytoskeleton (2,11–13).

An outstanding characteristic of desmosomes is their ability to acquire two different adhesive states in adaptation to differentiation-dependent and environmental cues (14,15). In their weaker state, which is present during junctional assembly and wound healing, desmosomes are Ca^{2+} dependent. In contrast, they acquire a strong and Ca^{2+}-independent state during maturation, which was

Submitted April 24, 2020, and accepted for publication September 8, 2020.
*Correspondence: franziska.vielmuth@med.uni-muenchen.de
Editor: Jason Swedlow.
https://doi.org/10.1016/j.bpj.2020.09.008

referred to as hyperadhesive (14,15). Importantly, cells are able to dynamically change from one state to the other and thus adapt quickly to changing environmental conditions, a fact that contributes to the importance of desmosomes in the maintenance of tissue integrity. Mechanistically, Garrod and Kimura suggested a model for desmosomal hyperadhesion, in which they propose that *cis* interactions of neighboring desmosomal cadherins capture Ca^{2+} ions between their extracellular domains and thus drive Ca^{2+} insensitivity (14,16). Further, regulation of hyperadhesion involves activity of protein kinase C-α and proper localization of Pkps (17), the latter of which also play a role in desmoglein clustering and desmosomal cadherin binding properties (18). Desmosomal hyperadhesion has so far been described as a characteristic that whole desmosomes acquire during their maturation, although the molecular mechanisms involved have not been elucidated. Challenging this hypothesis, desmosomal cadherins include four desmoglein (Dsg 1–4) and three desmocollin (Dsc 1–3) isoforms that show a tissue- and differentiation-specific expression (3,12). Interestingly, various isoform-specific functions of desmosomal cadherins have been reported, such as their respective involvement into signaling pathways and occurrence during morphogenesis (13,19–21). In accordance, we recently showed that Dsg1 and 3 binding properties and their regulation in keratinocytes are different (22,23). Thus, we here performed atomic force microscopy (AFM) on murine keratinocytes and chemical cross-linking experiments. We found different characteristics of Dsg1 and Dsg3 molecular binding properties during maturation, correlating with acquisition of hyperadhesion, which was paralleled with altered immunostaining characteristics of Dsg3 compared to Dsg1 in an ex vivo hyperadhesion model in human epidermis. These data indicate that Ca^{2+} independency in keratinocytes is paralleled by the modulation of binding of specific desmoglein isoforms such as Dsg3 on the molecular level.

MATERIALS AND METHODS

For detailed protocols regarding cell culture, immunostaining, and further experiments, please refer to Supporting Materials and Methods.

Hyperadhesion keratinocyte dissociation assay

Dispase assays were performed as described before (17). Cell monolayers were detached from the well bottom by a mixture of Dispase II (Sigma-Aldrich) and 1% collagenase I (Thermo Fisher Scientific). When monolayers were floating, enzymes were removed and substituted by complete FAD media without phenol red (0.05 mM $CaCl_2$). EGTA at a concentration of 5 mM was added for 90 min at 37°C and 5% CO_2. Afterwards, cell monolayers were exposed to a defined shear stress by pipetting with a 1 mL electrical pipette. Using a binocular microscope (Leica Microsystems, Mannheim, Germany), pictures were taken from resulting fragments. Counting of these fragments was done in ImageJ (National Institutes of Health, Bethesda, MD) using the analyze tool Analyze Particles. The fragment number represents an inverse measure for intercellular adhesion.

Purification of recombinant Dsg1- and 3-Fc construct

Recombinant human Dsg1- and 3-Fc proteins were purified as already described (24,25). In short, Dsg1- and Dsg3-Fc constructs contain the full extracellular domain of the corresponding Dsg isoform. Constructs were expressed in Chinese hamster ovarian cells. Isolation of recombinant proteins from the supernatants was performed using protein-A agarose affinity chromatography (Life Technologies, Carlsbad, CA).

AFM

For all measurements in this study, a NanoWizard 3 AFM (Bruker Nano, Berlin, Germany) connected to an inverted optical microscope (Carl Zeiss, Jena, Germany) was used. Cells were visualized through a 63× objective, which further allowed the selection of a scanning area. Topographic images as well as adhesion measurements were performed according to existing protocols (10,26). For quantitative imaging, we applied the following parameters: setpoint, 0.5 nN; Z-length, 2000 nm; and pulling speed, 50 μm/s; and for force mapping mode, the subsequent values were applied: setpoint, 0.5 nN; Z-length, 2000 nm; extend time, 0.2 ms; and delay in extended position (resting contact time), 0.1 s. In case of multievent binding during a retract cycle, we used for statistical analysis only the final unbinding event that led to the return of the cantilever to its neutral and undeflected position (27). Bar diagrams of the unbinding forces show the mean value of all median values of the cell borders. Lifetime of the bonds were determined by increasing the pulling speed stepwise from 1 to 20 μm/s. For analysis, unbinding force and loading rate values were determined by using the origins extreme fit distribution. Data points were fitted to a modified Bells equation as already done (10,28,29). For all experiments, we used the D-Tip (Si_3N_4) of MLCT cantilevers (Bruker, Mannheim, Germany), which have a tip radius of 20 nm and a nominal spring constant of 0.03 N/m. Functionalization of the tips to detect specific single molecule interactions was done via coating of the tips with a flexible heterobifunctional acetal-polyethylene glycol linker (Gruber Lab, Institute of Biophysics, Linz, Austria; BroadPharm, San Diego, CA for lifetime and energy barrier measurements) as stated elsewhere (30,31). Measurements were performed on MKZ cells in full FAD medium containing 1.2 mM Ca^{2+}.

Cross-linking, electrophoresis, and Western blot analysis

Membrane-impermeable cross-linking was performed as described elsewhere (9,18,32) and in Supporting Materials and Methods.

Tissue culture and human ex vivo hyperadhesion model

Biopsies of healthy human skin samples were performed as previously described (33). A written agreement for the use of research samples was obtained from all body donors as a part of the body donor program from the Institute of Anatomy and Cell Biology of the Ludwig-Maximilians-Universität München (München, Germany).

Data processing and statistics

For used software and applied statistics, please refer to the Supporting Materials and Methods.

RESULTS

Dsg3 single molecule binding is enhanced during acquisition of hyperadhesion

Keratinocytes in cell culture acquire a hyperadhesive state at a distinct time point of maturation (16). Thus, we investigated the time course during which murine keratinocytes become Ca^{2+} independent and thus hyperadhesive. Hyperadhesion keratinocytes dissociation assays in wild-type (wt) keratinocytes showed a significant decrease in fragmentation from 24 to 72 h in high Ca^{2+} medium, suggesting that wt cells become hyperadhesive after 72 h differentiation (Fig. 1, *A* and *B*). Next, we performed hyperadhesion keratinocyte dissociation assays at the same time points in Pkp-deficient keratinocytes as former studies showed that Pkps regulate Dsg3 binding properties (18), and Pkp1 is involved in desmosomal hyperadhesion (17). In contrast to wt keratinocytes, Pkp1- and 3-deficient keratinocytes failed to achieve Ca^{2+} independency after 72 h in high Ca^{2+} medium (Fig. 1, *A* and *B*), indicating that Pkps are required for desmosomal hyperadhesion. Underlining these data, immunostaining for Dsg3 and actin after EGTA incubation shows that Pkp1 and 3 both contribute to a proper localization of Dsg3 (Fig. S1, *A–C*).

We then applied AFM force measurements to investigate whether transition from the weak Ca^{2+} dependent state (24 h in high Ca^{2+} medium) to the strong hyperadhesive state (72 h in high Ca^{2+} medium) is accompanied by changes in desmosomal cadherin binding properties. Thus, we analyzed the single molecule binding properties of Dsg1 and Dsg3 as two representatives of the desmosomal cadherin family crucial for desmosomal adhesion in the epidermis as revealed by pemphigus disease in which they are targeted by autoantibodies (34). AFM tips were functionalized with recombinant Dsg3-Fc or Dsg1-Fc comprising the whole extracellular domains of the respective protein, and cells were examined after 24 and 72 h in high Ca^{2+} medium. Specificity of Dsg3 and Dsg1 interactions on murine keratinocytes was previously shown using inhibitory aDsg3 and aDsg1 antibodies (22,23).

AFM topography images showed no difference in cell morphology between different time points or several cell lines. All murine keratinocytes showed elevated cell borders (Fig. 1 *C*). We chose small areas along cell borders (5×2 μm) from AFM topography images and recorded adhesion maps (shown by *blue rectangles*). Every pixel represents an approach/retrace cycle of the AFM cantilever ran in force mapping mode. Gray value of pixels represent the topography at this respective position, whereas blue pixels depict a specific binding event.

For Dsg3, binding frequency was similar between 24 and 72 h in wt cell lines. Interestingly, binding frequency was reduced during the same time period in Pkp-deficient keratinocytes (Fig. 1 *D*), underlining their contribution to membrane availability of Dsg3 (18). Next, we evaluated the distribution ratio between Dsg3 binding events located at cell junctions and at nonjunctional areas. Here, we only observed a significant alteration for Pkp3-deficient cells comparing 24 and 72 h, but the same trend was observed for wt cell line (Fig. 1 *E*). Furthermore, we investigated the strength of Dsg3 single molecule interactions, referred to as unbinding force (UF). Importantly, the UF of wt cells significantly increased by 20% after 72 h in high Ca^{2+} medium compared to 24 h. In contrast, in Pkp1 and 3 knockout (k.o.) cells, UF was not significantly altered after differentiation (Fig. 1 *F*). Thus, Dsg3 molecules UFs in wt and Pkp-deficient keratinocytes clearly correlated with their ability to acquire a hyperadhesive state. This reflects a, to our knowledge, unreported phenomenon in which desmosomal hyperadhesion correlates with binding properties of a specific desmosomal cadherin. To characterize the measured bonds in more detail, we determined the bond lifetime for Dsg3 interactions. We therefore performed adhesion measurements at different pulling speeds ranging from 1 to 20 μm/s in wt murine keratinocytes. UF increased with increasing pulling speed at both time points, indicating that Dsg3 interactions in wt keratinocytes show a catch-bond behavior as reported earlier (10,23,35). Determination of bond lifetime for Dsg3 interactions was done by plotting the UF against the loading rate of the respective bond and fitting the values against a modified Bells equation (Fig. S2, *A* and *B*; (28,29)). Dsg3 bond lifetime for wt keratinocytes was increased from 1.38 to 3.52 s after 24 and 72 h, respectively (Fig. 1 *G*) and thus might be another correlate of desmosomal hyperadhesion. Interestingly, the unbinding position that was reported to be a measure for cytoskeletal anchorage (36) was not changed for wt cells comparing 24 and 72 h (Fig. S2 *C*), suggesting that cytoskeletal anchorage is not altered upon acquisition of hyperadhesion. Taken together, these results demonstrate increased UF and elongated bond lifetime of Dsg3 during acquisition of hyperadhesion in keratinocytes.

Dsg1 binding properties do not change during acquisition of hyperadhesion

In addition, we investigated the single molecule binding properties of the other main pemphigus antigen Dsg1. Comparable to Dsg3 measurements, yellow rectangles in the topography images show the adhesion maps (5 μm $\times$ 2 μm) and yellow dots mark specific binding events (Fig. 2 *A*). We observed a trend to decreased binding frequencies in all cell lines during differentiation, which was only significant in Pkp3-deficient keratinocytes (Fig. 2 *B*). The distribution ratio of Dsg1 binding events between 24 and 72 h was not changed in all cell lines (Fig. 2 *C*). Interestingly, Dsg1 single molecule UF was neither significantly altered

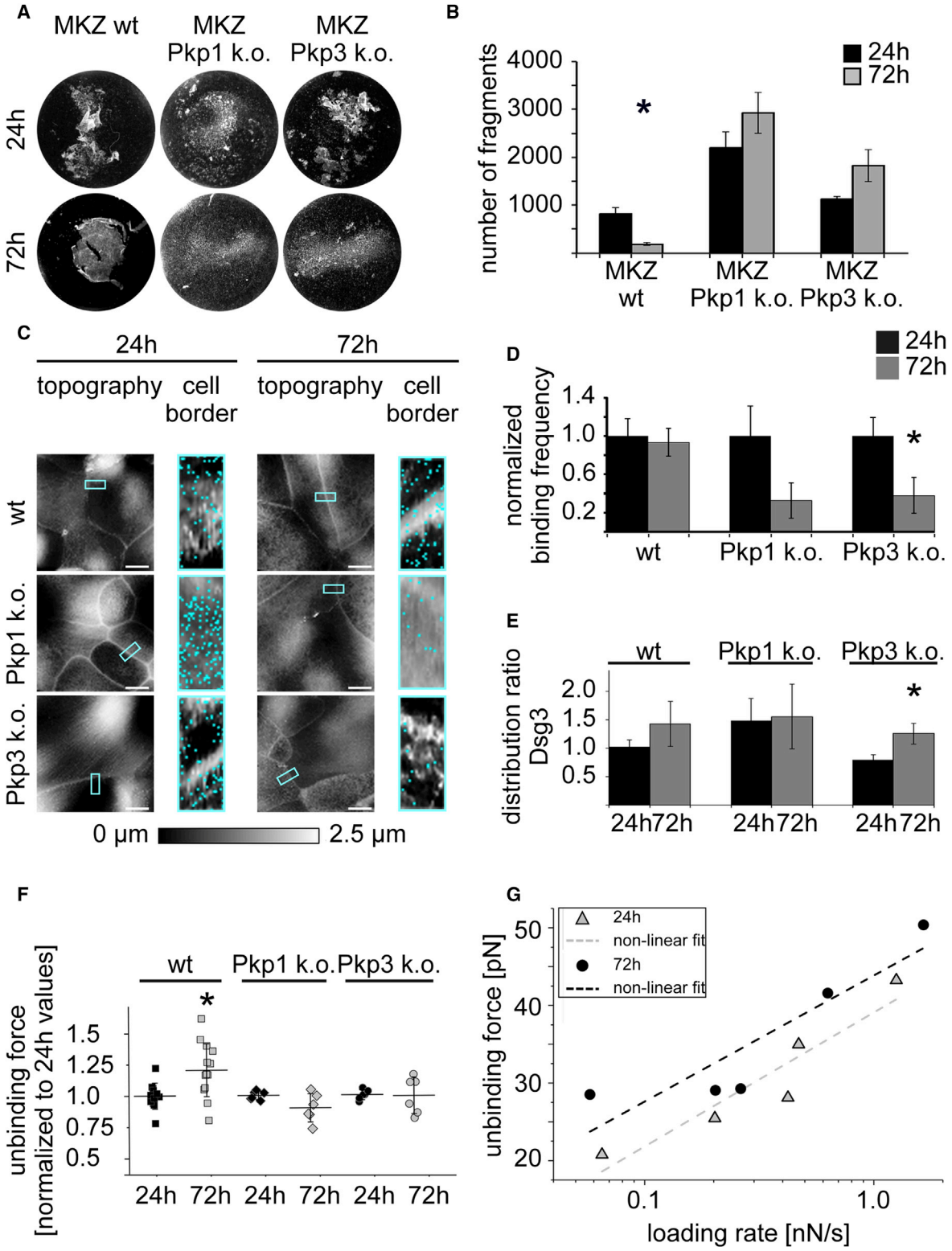

FIGURE 1 Dsg3 unbinding forces are increased in hyperadhesive wt keratinocytes. (*A*) Hyperadhesion dissociation assays in wt and Pkp1- and Pkp3-deficient murine keratinocytes are shown. Fragmentation after Ca^{2+} chelation after 72 h compared to 24 h in high Ca^{2+} medium was reduced for wt but not for Pkp-deficient keratinocytes, indicating that wt cells acquired a hyperadhesive state after 72 h differentiation. (*B*) Shown is quantification of dissociation assays ($n \geq 3$, $^*p < 0.05$ vs. 24 h). (*C*) AFM topography images show similar cell morphologies in wt, Pkp1 k.o., and Pkp3 k.o. cells after 24 and 72 h in high Ca^{2+} medium. Blue rectangles indicate areas of adhesion maps at cell borders, and blue dot represents one Dsg3 binding event. Scale bars, 10 μm. (*D*) Binding frequency is reduced in Pkp1- and significantly in Pkp3-deficient cells after 72 h of Ca^{2+} presence but not in wt. The binding frequency was normalized to the corresponding

(legend continued on next page)

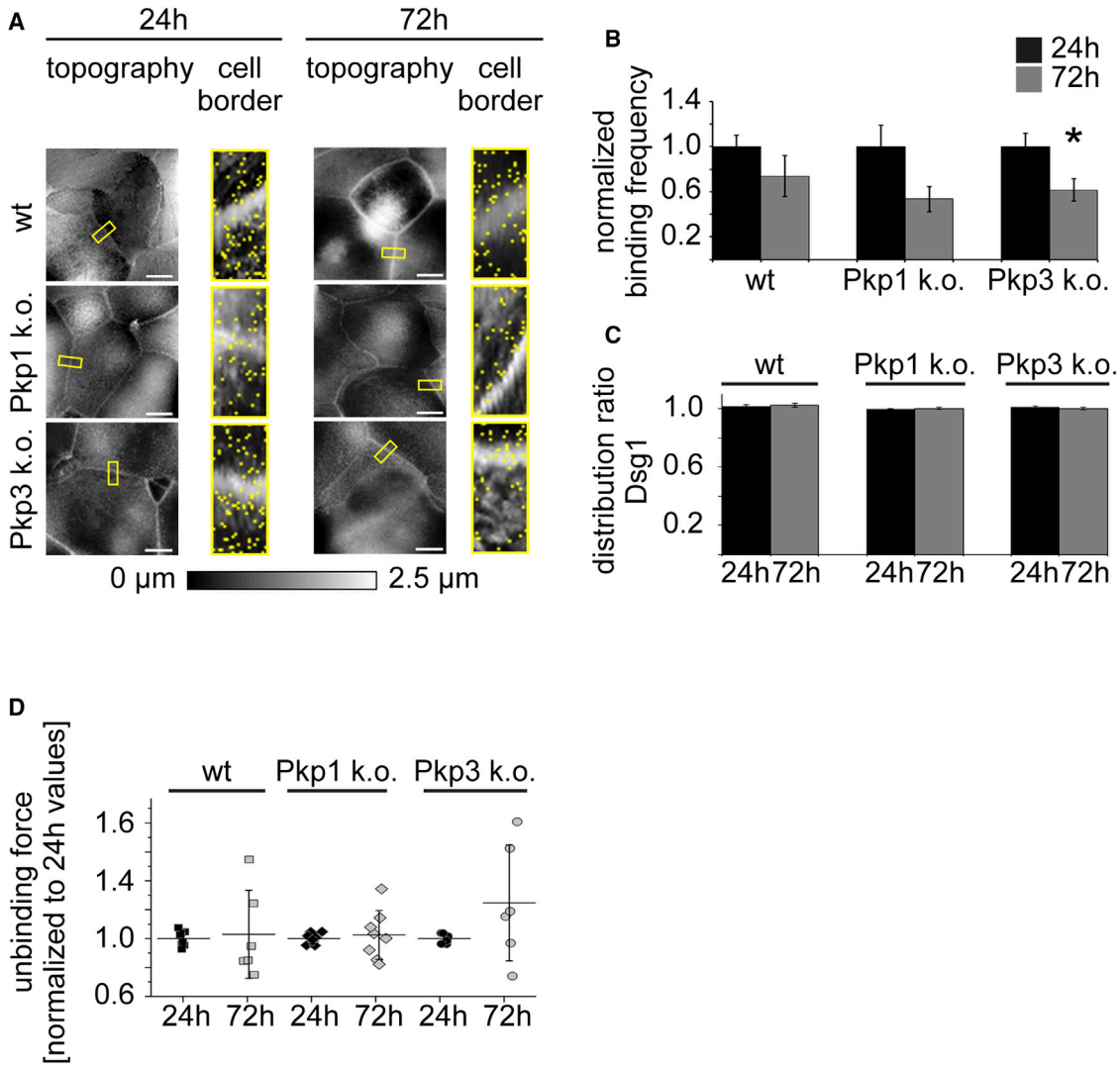

FIGURE 2 Binding properties of Dsg1 remain unchanged when keratinocytes become hyperadhesive. (*A*) All cell lines reveal similar cell morphology after 24 and 72 h in high Ca^{2+} medium as shown by AFM topography images. Yellow rectangles indicate areas of adhesion maps at cell borders, and every yellow dot describes one Dsg1 binding event. Scale bars, 10 μm. (*B*) Binding frequency is significantly reduced in Pkp3-deficient cells after 72 h of Ca^{2+} presence only. The binding frequency was normalized to the corresponding 24 h values. (*C*) Distribution ratio between junctional and perijunctional compartment is not altered between 24 and 72 h of maintenance in high Ca^{2+} medium. (*D*) Dsg1 single molecule unbinding strength is not significantly changed in all cell lines after 72 h in high Ca^{2+} medium. UF was calculated using the mean of single medians. (*B–D*) $n = 3$ with two cell borders/experiment and 1000 force curves per measured cell border; error bars represent standard error of the mean (*$p < 0.05$ vs 24 h).

after 72 h in high Ca^{2+} medium in wt nor in Pkp-deficient keratinocytes when compared to 24 h (Fig. 2 *D*), indicating that Dsg1 shows another differentiation-dependent behavior during the acquisition of hyperadhesion then Dsg3. According to Dsg3 interactions, the unbinding position was not significantly altered between both time points in wt (Fig. S2 *B*). Taken together, these data show that contribution of single molecule binding properties to desmosomal hyperadhesion differs between Dsg1 and Dsg3 in this specific time interval.

Desmosomal hyperadhesion correlates with increased Dsg3 clustering

Clustering of desmosomal molecules was suggested to be one mechanism underlying desmosomal hyperadhesion

24 h values. (*E*) Dsg3 distribution ratio between junctional and perijunctional compartments shows significant differences for Pkp3-deficient cells between both time points but not for wt and Pkp1 k.o. cells. (*F*) Dsg3 single molecule UF is increased in wt cells after 72 h of Ca^{2+} compared to 24 h. In contrast, Pkp1 and Pkp3 k.o. cells lack an increase in Dsg3 UF. UF was calculated using the mean of single medians. (*D–F*) $n \geq 3$ with two cell borders/experiment and 1000 force curves per measured cell border; error bars represent standard error (*$p < 0.05$ vs 24 h). (*G*) Fitting of peaks of UF versus peaks of loading rates shows a linear increase with logarithm after 24 and 72 h in high Ca^{2+} medium. $n = 8$ with two cell borders/experiment and 100 force curves per measured cell border.

(37). This is conclusive with regards to densely packed desmosomes in the epidermis (3,38,39). Desmosomal clustering can be studied indirectly by membrane-impermeable cross-linking, which demonstrates Dsg oligomerization (9,18). Thus, we checked for Ca^{2+}-insensitive Dsg oligomers after 24 and 72 h in high Ca^{2+} medium by treatment with 5 mM EGTA for 90 min. In wt murine keratinocytes, the amount of Ca^{2+} independent Dsg3 oligomers was significantly increased from 24 to 72 h (Fig. 3, *A* and *B*), suggesting that Dsg3 oligomers contribute to hyperadhesion. Interestingly, this increase occurs in parallel with an increased UF and an elongated bond lifetime of Dsg3 during the acquisition of hyperadhesion. These data indicate that Dsg3 contributes to desmosomal hyperadhesion not only via changing its single molecule binding properties but also by increased occurrence of Ca^{2+} independent oligomers.

Recent results showed that Pkp1 is important for clustering of Dsg3 (18), Thus, we next investigated the effect of Pkp deficiency on Ca^{2+} dependent Dsg3 oligomerization. In Pkp1-deficient keratinocytes, the amount of Dsg3 oligomers was drastically reduced compared to wt without EGTA treatment at both time points. Furthermore, as shown by oligomerization ratio, Ca^{2+}-insensitive Dsg3 oligomers do not significantly increase in Pkp1-deficient keratinocytes after 72 h (Fig. 3, *A* and *B*). These data indicate that Pkp1 deficiency diminishes the acquisition of hyperadhesion by changes in Dsg3 oligomerization and thus underline the importance of both Pkp1 presence and Dsg3 oligomerization for desmosomal hyperadhesion.

In contrast, Ca^{2+} independent Dsg3 oligomers were reduced in Pkp3 k.o. cells after 24 h but increased from 24 to 72 h. Even though the increase was to a minor extent compared with wt cells, this result shows that Pkp3 is less relevant for desmosomal cadherin oligomerization (Fig. 3, *A* and *B*). Taken together, these findings suggest that Pkp1 but not Pkp3 contributes to desmosomal hyperadhesion via clustering of Dsg3.

We further checked for other desmosomal cadherins regarding their Ca^{2+} independent oligomerization. The amount of Dsg1 oligomers was minor for all cell lines at both time points compared with Dsg3 (Fig. 3 *C*). However, there were at least some Ca^{2+} independent Dsg1 oligomers in all cell lines at both time points (Fig. 3 *D*). In addition, the amount was not altered during differentiation, which is in concordance to unchanged Dsg1 single molecule binding properties shown above (Fig. 2, *C* and *D*). Interestingly, Pkp1-deficient cells almost completely lost their Dsg1 expression after 72 h, whereas Dsg1 expression was drastically increased in the wt cell line, indicating that Pkp1 is important for proper expression of Dsg1 during differentiation.

Hyperadhesion was referred to be a special feature of desmosomes and thus should not be present for classical cadherins in adherens junctions (16). Thus, we evaluated the occurrence of Ca^{2+}-insensitive oligomers of the classical cadherin E-cadherin (E-Cad). Accordingly, treatment with EGTA led to a complete disappearance of E-Cad oligomers in all cell lines, showing that E-Cad remains Ca^{2+} dependent during maturation (Figs. 3 *E* and S3 *A*) and confirming that hyperadhesion is a specific feature of desmosomes. To further underline the Ca^{2+} dependency of E-Cad, we did a comparison between EGTA-treated and control oligomer bands (Fig. S3 *A*).

These results demonstrate different Dsg1 and Dsg3 clustering during differentiation and thus underline the different contribution of desmosomal cadherin isoforms in the acquisition of hyperadhesion.

Ex vivo models reveal distinct Ca^{2+} dependency of Dsg1 and 3 immunostaining characteristics

Previous studies proposed that all desmosomes in mature epidermis are hyperadhesive and thus Ca^{2+} independent regardless of their composition (15,16,40). With regards to the observed differences for Dsg1 and 3 during differentiation, we tested the Ca^{2+} dependency of several desmosomal cadherin isoforms in a human ex vivo model. To do so, human skin samples from body donors were incubated with the Ca^{2+} chelator EGTA for 1.5 or 24 h, respectively. Subsequently, skin sections were stained for Dsg1 or Dsg3. Viability of the tissue was confirmed in previous studies (33).

According to previous results, Dsg1 and 3 showed different expression gradients in human epidermis with Dsg1 being predominant in superficial epidermis, whereas Dsg3 is more abundant in the basal epidermal layers (Fig. 4, *A* and *B*). EGTA treatment for 1.5 h had no effect on Dsg1 and 3 expression along keratinocyte cell membranes in human epidermis (Fig. 4, *A*, *B*, and *E*). In contrast, EGTA incubation for 24 h led to a fragmentation, reduction, and confinement to small dots of Dsg1 staining throughout all epidermal layers (Fig. 4, *C* and *F*). On the contrary, Dsg3 staining was not altered after 24 h of EGTA treatment (Fig. 4, *D* and *F*). These results argue for a distinct behavior of desmosomal cadherins in human epidermis in which Dsg3 is largely Ca^{2+} independent, whereas Dsg1 remains at least in part Ca^{2+} dependent. Taken together, these data suggest a stronger Ca^{2+} independency of Dsg3 immunostaining compared to Dsg1 in the human epidermis.

To test whether Dsc show different Ca^{2+} dependent immunostaining as well, we stained the human epidermis for Dsc1 and Dsc3 after 1.5 and 24 h of EGTA incubation. Interestingly, Dsc1 showed no overall reduction in staining after 1.5 but a significant change after 24 h EGTA treatment. Further, staining along cell borders after 24 h of EGTA treatment was broadened and showed a partly cytosolic pattern. These data, similarly to Dsg1, indicate that Dsc1 is at least in part Ca^{2+} dependent. In contrast, Dsc3 staining showed

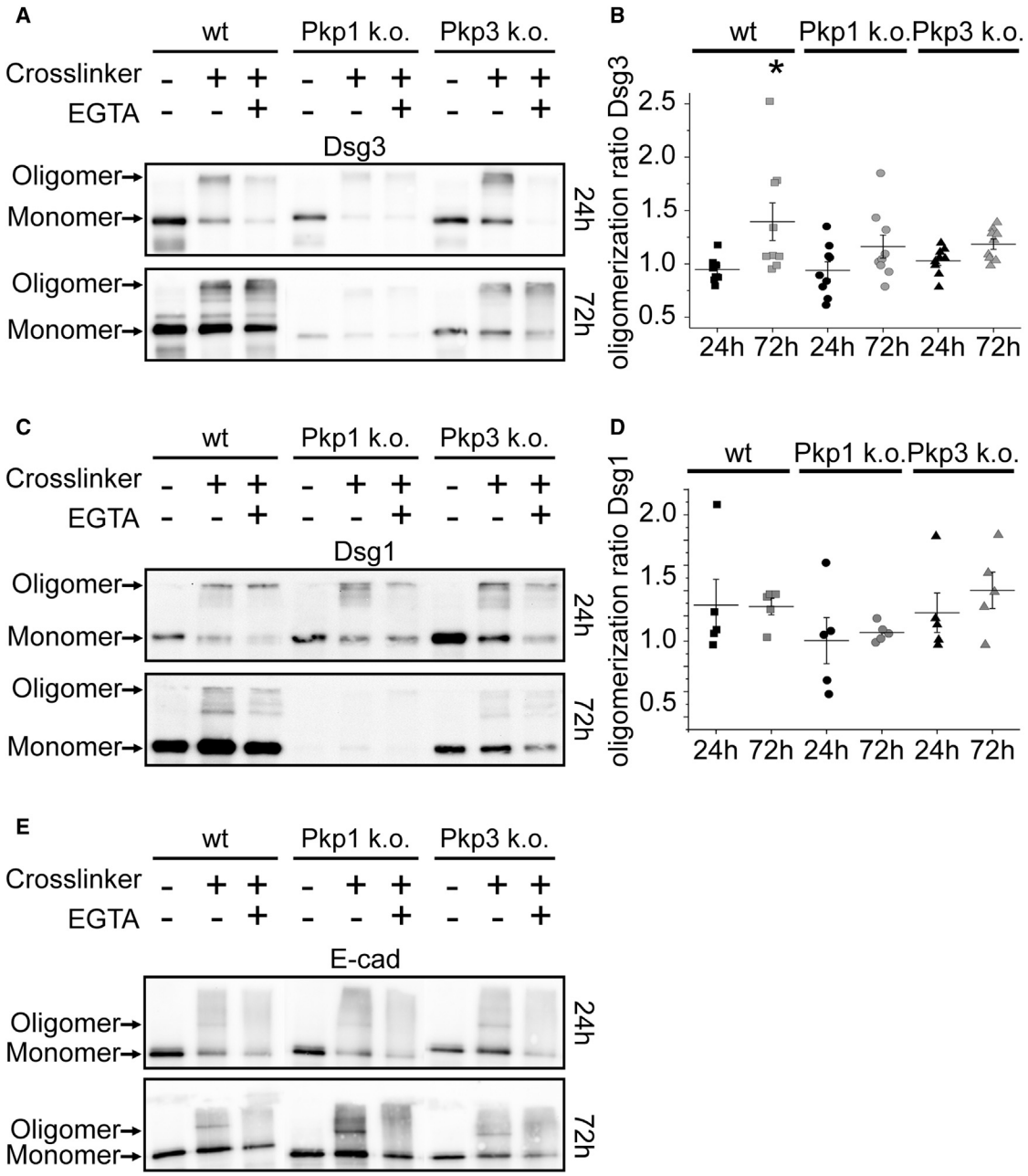

FIGURE 3 Pkp1-dependent Dsg3 oligomerization correlates with the development of a hyperadhesive state in murine keratinocytes. Cells were treated with EGTA (5 mM for 90 min at 37°C) after 24 or 72 h in high Ca^{2+} medium followed by chemical cross-linking with ethylene glycol bis(sulfosuccinimidyl succinate). Cell lysates were prepared after standard protocol. (*A*) Wt and Pkp3-deficient keratinocytes show increased Ca^{2+} independent Dsg3 oligomers after 72 h compared to 24 h in high Ca^{2+} medium. In contrast, almost no Ca^{2+} independent Dsg3 oligomers develop in Pkp1-deficient keratinocytes. (*B*) Ratio of oligomerization reveals a significantly increased number of Ca^{2+} independent Dsg3 oligomers after 72 h compared to 24 h in wt keratinocytes. Error bars represent standard error of the mean ($n = 9$, $^*p < 0.05$ vs. 24 h). (*C*) The extent of Ca^{2+} independent Dsg1 oligomers was smaller in all cell lines after 24 h as well as after 72 h in high Ca^{2+} medium, although total protein amount was drastically increased after 72 h in wt keratinocytes. (*D*) Ratio of oligomerization reveals no significantly increased number of Ca^{2+} independent Dsg1 oligomers after 72 h compared to 24 h in all cell lines. Error bars represent standard error of the mean ($n = 5$). (*E*) Western blot shows that E-Cad oligomers are Ca^{2+} dependent after both 24 and 72 h maintenance in high Ca^{2+} medium. All Western blots are representative of $n = 5$.

no overall reduction after 1.5 or 24 h EGTA incubation. Thus, Dsc3 and Dsg3 reveal similarity in their Ca^{2+} independency (Fig. S3, *B–G*). To exclude that these results are caused by shedding of desmosomal cadherins or changes in antibody epitope binding by EGTA treatment, we performed all experiments with a second set of primary antibodies (Table S1). These experiments confirmed the results shown above (Fig. S4, *A–D*).

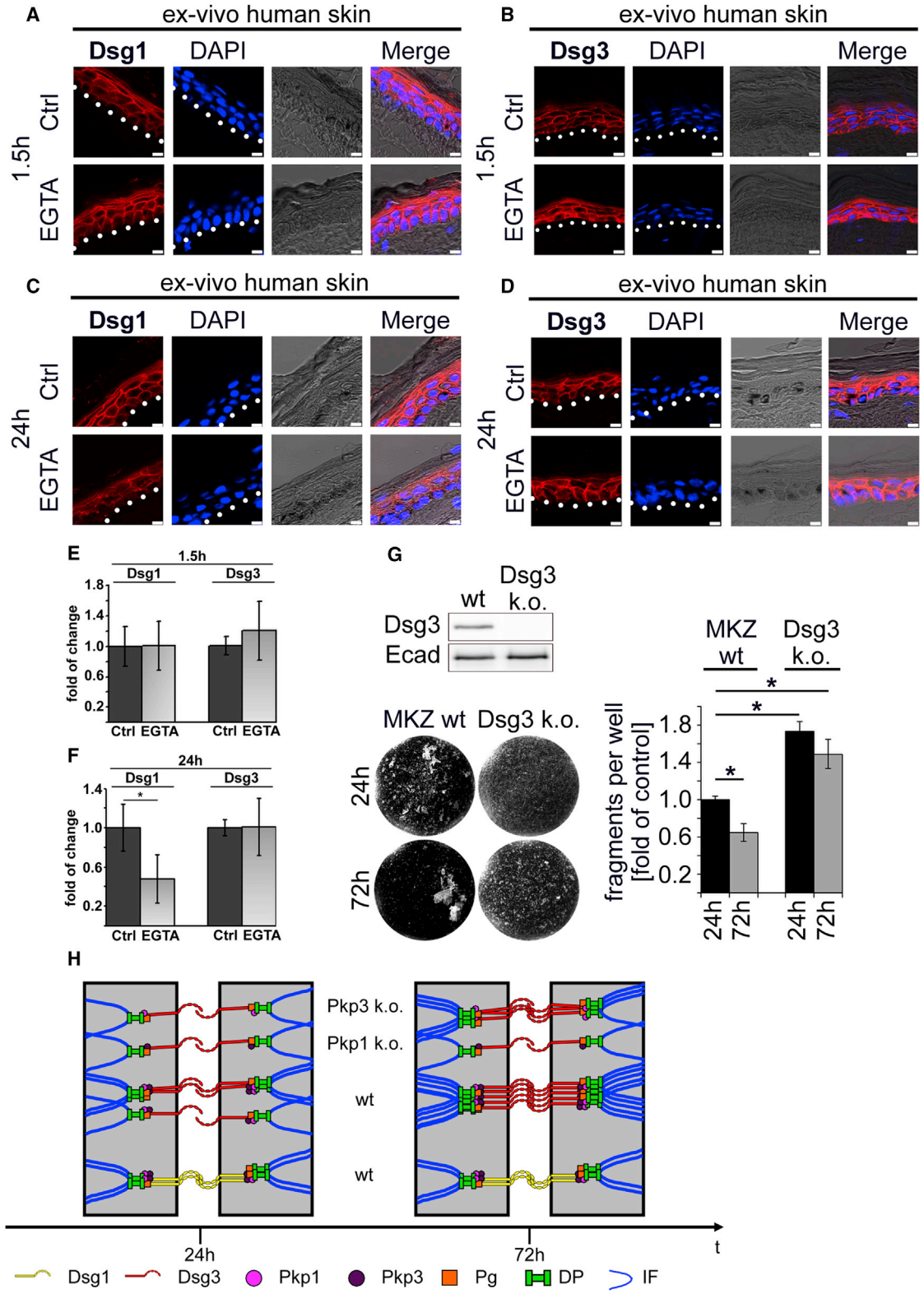

FIGURE 4 Dsg3 is hyperadhesive in human epidermis. (*A* and *B*) 1.5 h of EGTA incubation showed no alterations of Dsg1 and Dsg3 staining in human ex vivo skin samples. (*C*) Treatment of EGTA for 24 h led to a fragmentation of Dsg1 throughout all human epidermal layers. Dsg1 staining is drastically reduced and confined to small dots at cell membranes. (*D*) In contrast to Dsg1, Dsg3 staining in human epidermis is not altered after 24 h of EGTA treatment. (*A–D*) Scale bars, 7.5 μm. (*E* and *F*) Quantification of Dsg1 and Dsg3 staining after 1.5 and 24 h of EGTA incubation shows a significant decrease for Dsg1 staining after 24 h between control and EGTA treatment, whereas 1.5 h EGTA treatment led to no change. $n \geq 4$ different body donors; error bars represent

(legend continued on next page)

Keratinocytes lacking Dsg3 fail to become hyperadhesive

To investigate the influence of a specific desmosomal cadherin isoform for desmosomal hyperadhesion, we conducted hyperadhesion keratinocyte dissociation assays in murine keratinocytes lacking Dsg3 (Fig. 4 *G*). According to our previous results, Dsg3-deficient keratinocytes in contrast to wt cells failed to acquire a hyperadhesive and thus Ca^{2+} independent state during the given differentiation time period (Fig. 4 *G*). This shows the importance of Dsg3 for desmosomal hyperadhesion.

Taken together, the data show that different desmosomal cadherin isoforms contribute to desmosomal hyperadhesion by distinct mechanisms. Our experiments demonstrate for the first time, to our knowledge, that acquisition of desmosomal hyperadhesion correlates with alterations in clustering as well as single molecule binding properties of specific desmosomal cadherins such as Dsg3.

DISCUSSION

Dsg3 single molecule binding properties provide insights into molecular mechanisms contributing to the acquisition of hyperadhesion

Hyperadhesion is a cell-cell adhesion concept that refers to the strong adhesive state of desmosomes (14,15). In mature epidermis, most desmosomes were characterized as hyperadhesive, which seem to be crucial for strong cell cohesion and to withstand mechanical shear stress (14,37). In contrast, desmosomes were described to be in a weaker and Ca^{2+} dependent state during assembly and wound healing (40). Thus, desmosomes switch between the two adhesive states. Apart from tissue (41), also, desmosomes in cell culture models can acquire the hyperadhesive state during maturation (42,43). In pemphigus vulgaris, a blistering skin disease in which autoantibodies against Dsg1 and 3 affect cell cohesion, experiments with hyperadhesive keratinocytes showed less disturbance of intercellular contacts and internalization of the adhesion molecules (44). Hence, hyperadhesion is a very important property of keratinocytes, for example to reduce susceptibility for diseases. In cell culture models, chelation of Ca^{2+} ions provides an approach to investigate Ca^{2+} independency of desmosomes. In our model, murine keratinocytes acquire a hyperadhesive state within 72 h in high Ca^{2+} medium. Mechanistically, hyperadhesion was attributed to organized desmosomal cadherins, which capture Ca^{2+} ions via *cis* binding between their extracellular domains (14,15). However, the contribution of certain desmosomal cadherins remains unclear.

Because hyperadhesion is thought to be a strong adhesive state, we performed AFM experiments investigating single molecule binding properties of desmosomal cadherins (10,45–47). Here, we measured single molecule interactions of Dsg1 and 3 under nonhyperadhesive and hyperadhesive conditions in murine keratinocytes. Binding properties for Dsg3 were drastically altered when cells reached a hyperadhesive state, whereas no changes were observed for Dsg1. Interestingly, different regulations of Dsg1 and 3 binding properties were determined before (23). The frequencies of Dsg1 and 3 interactions were slightly reduced for wt and Pkp1 k.o. cells between 24 and 72 h in high Ca^{2+} medium and dropped significantly in Pkp3 k.o. cells. Those results confirm former results that Pkp3 is relevant for desmosome assembly during maturation (17,48,49). Therefore, Pkp3 may contribute to desmosomal hyperadhesion via this mechanism, whereas Pkp1 may primarily control clustering of Dsg3. Interestingly, we found that unbinding forces of Dsg3 interactions increased from 24 to 72 h in high Ca^{2+} medium for wt but not for Pkp-deficient keratinocytes, whereas Dsg1 unbinding forces showed no significant alterations for all cell lines at both time points. Higher unbinding forces of Dsg3 interactions were shown to correlate with the strengthening of overall intercellular adhesion and thus fit to the acquirement of a hyperadhesive state (10,23). Changes in Dsg3 unbinding forces may also be due to participation of more Dsg3 molecules as we use Fc-tagged Dsg3 extracellular domains to functionalize AFM cantilevers. This would be in line with increased clustering of Dsg3 after 72 h in high Ca^{2+} medium and thus an enhanced possibility of multiple bindings because of a higher Dsg3 molecule density. However, former data on cadherin-mediated adhesion indicate that multiple molecules participating in a certain unbinding event cause unbinding forces that are multiples of the single molecule unbinding strength (35,50). In contrast, UF only increased by 20% in our data, suggesting changes in the single molecule binding to be more likely.

Furthermore, acquisition of the hyperadhesive state seems to have an isoform-specific timeline. For Dsg3 but not for Dsg1, we found changes in its single molecules properties between 24 and 72 h. Nevertheless, data using Dsg2 k.o. cells argue for a contribution of all desmosomal cadherins to desmosomal hyperadhesion. Thus, it can be speculated that Dsg1 binding properties may change during another time period in the differentiation process. An explanation for this observation could be found in the epidermis

the SD (*$p < 0.05$ versus respective control). (*G*) Representative Western blot confirms complete k.o. of Dsg3 in murine keratinocyte cell lines. After 72 h in high Ca^{2+} medium, cells lacking Dsg3 fail to become hyperadhesive as shown by the high degree of fragmentation compared to wt cells after 72 h in high Ca^{2+} medium. $n = 3$ ($p < 0.05$ vs. wt 24 h). (*H*) Mechanistic model of the experimental findings is shown. Dsg1 clusters remain unaltered for wt cells under nonhyperadhesive and hyperadhesive conditions, whereas Dsg3 clusters are increased and UF is enhanced. In Pkp3-deficient cells, Dsg3 is still able to cluster, even though the UF remains unchanged. In contrast, Pkp1 deficiency abrogates proper clustering of Dsg3.

where Dsg1 is more prominent in the superficial layers. Therefore, Dsg1 properties may change late during differentiation. Further studies are necessary for a deeper understanding of this process.

Dsg3 interactions behave like catch bonds at both adhesive states, which fits former studies (10,51). However, Dsg3 bond lifetime was prolonged when cells become hyperadhesive. Bond lifetime at 24 h in high Ca^{2+} medium was similar as shown before for desmosomal cadherins, whereas the lifetime increased during 72 h in high Ca^{2+} medium and reaches levels known for classical cadherins (10,35,52). Interestingly, Dsg3 molecules unbinding forces are also increased during this time period, suggesting that altered forces and bond lifetimes may be interdependent (53). Moreover, the data indicate that changes in single molecules binding properties of Dsg3 contribute to desmosomal hyperadhesion.

Desmosomal clustering correlates with hyperadhesion and is mediated by Pkp1

Previous studies showed the importance of Pkps for desmosomal hyperadhesion as well as for clustering of desmosomal cadherins (17,18,54). Further, desmosomes require organized desmosomal proteins to become hyperadhesive (14). As previously shown, clustering of Dsg3 is mediated by Pkp1 but not Pkp3. Here, we observed that Ca^{2+} independent Dsg3 oligomers correlate with desmosomal hyperadhesion and require Pkp 1. In contrast, Dsg1 demonstrated a minor extent of Ca^{2+} independent oligomers. However, this reduced amount of Ca^{2+} independent oligomers remained unchanged after 24 and 72 h in wt murine keratinocytes. This finding supports the AFM data, in which no differences in single molecule binding properties of Dsg1 were observed during this time frame. Hence, we propose that oligomerization of desmosomal proteins is a correlate of desmosomal hyperadhesion, which occurs for desmosomal cadherins during different time intervals.

Specific desmosomal cadherins show different Ca^{2+} dependencies in human epidermis

Finally, we show that Dsg1 immunostaining is less resistant to Ca^{2+} chelation compared to Dsg3 in human epidermis by the usage of ex vivo models and application of EGTA. The fact that Dsg3 distribution patterns as revealed by immunostaining are resistant to Ca^{2+} chelation whereas Dsg1 staining properties are not indicates a further isoform specificity of desmosomal cadherins in the desmosome. This is in line with former studies providing evidence for different functions of desmosomal cadherin isoforms (19–21,32). Further desmosomal cadherins are differentially expressed throughout the epidermis (3,39,55). Thus, it is conclusive that they engage different functions during tissue maturation and hyperadhesion.

CONCLUSION

In this study, we investigated the acquisition of hyperadhesion in murine keratinocytes and the Ca^{2+} dependency of desmosomal cadherins in human epidermis by AFM, biochemical cross-linking, and immunostaining experiments. Our data show a, to our knowledge, unreported phenomenon that during acquisition of desmosomal hyperadhesion, desmosomal cadherins undergo an isoform-specific process and thus contribute to desmosomal hyperadhesion via several mechanisms, including desmosomal clustering and increased molecules binding strength. Further, the acquisition of this state depends on Pkps. We demonstrate that desmosomal cadherin clustering, which requires Pkp1, correlates with hyperadhesion. On a single molecule level, we detected an increase in the Dsg3 molecules unbinding force and interaction lifetime as a correlate for desmosomal hyperadhesion. Taken together, the data suggest that desmosomal hyperadhesion is paralleled by alterations of specific desmosomal cadherin binding properties such as changes in clustering and molecules binding strength (Fig. 4 *H*).

SUPPORTING MATERIAL

Supporting Material can be found online at https://doi.org/10.1016/j.bpj.2020.09.008.

AUTHOR CONTRIBUTIONS

M.F. conducted experiments, acquired data, and analyzed data. M.F. and A.S. determined methodology. F.V. and J.W. designed research studies. M.F., F.V., and J.W. wrote the manuscript.

ACKNOWLEDGMENTS

We thank Andrea Wehmeyer, Nadine Albrecht, Sabine Mühlsimer, and Martina Hitzenbichler for excellent technical assistance and JPK Instruments for constructive discussion. We thank Mechthild Hatzfeld and Rene Keil for providing the MKZ cell lines.

The project is funded by Else Kröner-Fresenius-Stiftung 2016_AW157 to F.V. and J.W., Deutsche Forschungsgemeinschaft VI 921/2-1 to F.V., and Deutsche Forschungsgemeinschaft WA2474/10-2 to J.W.

REFERENCES

1. Price, A. J., A.-L. Cost, …, C. Grashoff. 2018. Mechanical loading of desmosomes depends on the magnitude and orientation of external stress. *Nat. Commun.* 9:5284.
2. Hatzfeld, M., R. Keil, and T. M. Magin. 2017. Desmosomes and intermediate filaments: their consequences for tissue mechanics. *Cold Spring Harb. Perspect. Biol.* 9:a029157.
3. Delva, E., D. K. Tucker, and A. P. Kowalczyk. 2009. The desmosome. *Cold Spring Harb. Perspect. Biol.* 1:a002543.
4. Spindler, V., and J. Waschke. 2018. Pemphigus—a disease of desmosome dysfunction caused by multiple mechanisms. *Front. Immunol.* 9:136.

5. Pollmann, R., T. Schmidt, …, M. Hertl. 2018. Pemphigus: a comprehensive review on pathogenesis, clinical presentation and novel therapeutic approaches. *Clin. Rev. Allergy Immunol.* 54:1–25.
6. McGrath, J. A., J. R. McMillan, …, R. A. Eady. 1997. Mutations in the plakophilin 1 gene result in ectodermal dysplasia/skin fragility syndrome. *Nat. Genet.* 17:240–244.
7. Winik, B. C., R. A. Asial, …, M. C. Boente. 2009. Acantholytic ectodermal dysplasia: clinicopathological study of a new desmosomal disorder. *Br. J. Dermatol.* 160:868–874.
8. Harrison, O. J., J. Brasch, …, L. Shapiro. 2016. Structural basis of adhesive binding by desmocollins and desmogleins. *Proc. Natl. Acad. Sci. USA.* 113:7160–7165.
9. Nie, Z., A. Merritt, …, D. Garrod. 2011. Membrane-impermeable cross-linking provides evidence for homophilic, isoform-specific binding of desmosomal cadherins in epithelial cells. *J. Biol. Chem.* 286:2143–2154.
10. Vielmuth, F., V. Spindler, and J. Waschke. 2018. Atomic force microscopy provides new mechanistic insights into the pathogenesis of pemphigus. *Front. Immunol.* 9:485.
11. Hobbs, R. P., and K. J. Green. 2012. Desmoplakin regulates desmosome hyperadhesion. *J. Invest. Dermatol.* 132:482–485.
12. Waschke, J. 2008. The desmosome and pemphigus. *Histochem. Cell Biol.* 130:21–54.
13. Waschke, J., and V. Spindler. 2014. Desmosomes and extradesmosomal adhesive signaling contacts in pemphigus. *Med. Res. Rev.* 34:1127–1145.
14. Garrod, D., and T. E. Kimura. 2008. Hyper-adhesion: a new concept in cell-cell adhesion. *Biochem. Soc. Trans.* 36:195–201.
15. Garrod, D. R., M. Y. Berika, …, L. Tabernero. 2005. Hyper-adhesion in desmosomes: its regulation in wound healing and possible relationship to cadherin crystal structure. *J. Cell Sci.* 118:5743–5754.
16. Garrod, D., and L. Tabernero. 2014. Hyper-adhesion: a unique property of desmosomes. *Cell Commun. Adhes.* 21:249–256.
17. Keil, R., K. Rietscher, and M. Hatzfeld. 2016. Antagonistic regulation of intercellular cohesion by plakophilins 1 and 3. *J. Invest. Dermatol.* 136:2022–2029.
18. Fuchs, M., M. Foresti, …, F. Vielmuth. 2019. Plakophilin 1 but not plakophilin 3 regulates desmoglein clustering. *Cell. Mol. Life Sci.* 76:3465–3476.
19. Walter, E., F. Vielmuth, …, J. Waschke. 2019. Role of Dsg1- and Dsg3-mediated signaling in pemphigus autoantibody-induced loss of keratinocyte cohesion. *Front. Immunol.* 10:1128.
20. Valenzuela-Iglesias, A., H. E. Burks, …, K. J. Green. 2019. Desmoglein 1 regulates invadopodia by suppressing EGFR/Erk signaling in an erbin-dependent manner. *Mol. Cancer Res.* 17:1195–1206.
21. Waschke, J. 2019. Desmogleins as signaling hubs regulating cell cohesion and tissue/organ function in skin and heart - EFEM lecture 2018. *Ann. Anat.* 226:96–100.
22. Vielmuth, F., E. Walter, …, J. Waschke. 2018. Keratins regulate p38MAPK-dependent desmoglein binding properties in pemphigus. *Front. Immunol.* 9:528.
23. Vielmuth, F., M. T. Wanuske, …, V. Spindler. 2018. Keratins regulate the adhesive properties of desmosomal cadherins through signaling. *J. Invest. Dermatol.* 138:121–131.
24. Heupel, W. M., D. Zillikens, …, J. Waschke. 2008. Pemphigus vulgaris IgG directly inhibit desmoglein 3-mediated transinteraction. *J. Immunol.* 181:1825–1834.
25. Waschke, J., P. Bruggeman, …, D. Drenckhahn. 2005. Pemphigus foliaceus IgG causes dissociation of desmoglein 1-containing junctions without blocking desmoglein 1 transinteraction. *J. Clin. Invest.* 115:3157–3165.
26. Vielmuth, F., E. Hartlieb, …, V. Spindler. 2015. Atomic force microscopy identifies regions of distinct desmoglein 3 adhesive properties on living keratinocytes. *Nanomedicine (Lond.).* 11:511–520.
27. Baumgartner, W., P. Hinterdorfer, and H. Schindler. 2000. Data analysis of interaction forces measured with the atomic force microscope. *Ultramicroscopy.* 82:85–95.
28. Bell, G. I. 1978. Models for the specific adhesion of cells to cells. *Science.* 200:618–627.
29. Wieland, J. A., A. A. Gewirth, and D. E. Leckband. 2005. Single molecule adhesion measurements reveal two homophilic neural cell adhesion molecule bonds with mechanically distinct properties. *J. Biol. Chem.* 280:41037–41046.
30. Ebner, A., L. Wildling, …, H. J. Gruber. 2007. A new, simple method for linking of antibodies to atomic force microscopy tips. *Bioconjug. Chem.* 18:1176–1184.
31. Wildling, L., B. Unterauer, …, H. J. Gruber. 2011. Linking of sensor molecules with amino groups to amino-functionalized AFM tips. *Bioconjug. Chem.* 22:1239–1248.
32. Hartlieb, E., B. Kempf, …, J. Waschke. 2013. Desmoglein 2 is less important than desmoglein 3 for keratinocyte cohesion. *PLoS One.* 8:e53739.
33. Egu, D. T., E. Walter, …, J. Waschke. 2017. Inhibition of p38MAPK signalling prevents epidermal blistering and alterations of desmosome structure induced by pemphigus autoantibodies in human epidermis. *Br. J. Dermatol.* 177:1612–1618.
34. Schmidt, E., M. Kasperkiewicz, and P. Joly. 2019. Pemphigus. *Lancet.* 394:882–894.
35. Baumgartner, W., P. Hinterdorfer, …, D. Drenckhahn. 2000. Cadherin interaction probed by atomic force microscopy. *Proc. Natl. Acad. Sci. USA.* 97:4005–4010.
36. Sariisik, E., C. Popov, …, M. Benoit. 2015. Decoding cytoskeleton-anchored and non-anchored receptors from single-cell adhesion force data. *Biophys. J.* 109:1330–1333.
37. Kimura, T. E., A. J. Merritt, …, D. R. Garrod. 2012. Desmosomal adhesiveness is developmentally regulated in the mouse embryo and modulated during trophectoderm migration. *Dev. Biol.* 369:286–297.
38. Kowalczyk, A. P., and K. J. Green. 2013. Structure, function, and regulation of desmosomes. *Prog. Mol. Biol. Transl. Sci.* 116:95–118.
39. Green, K. J., A. Jaiganesh, and J. A. Broussard. 2019. Desmosomes: essential contributors to an integrated intercellular junction network. *F1000Res.* 8:F1000 Faculty Rev-2150.
40. Wallis, S., S. Lloyd, …, D. Garrod. 2000. The alpha isoform of protein kinase C is involved in signaling the response of desmosomes to wounding in cultured epithelial cells. *Mol. Biol. Cell.* 11:1077–1092.
41. Borysenko, J. Z., and J. P. Revel. 1973. Experimental manipulation of desmosome structure. *Am. J. Anat.* 137:403–421.
42. Kimura, T. E., A. J. Merritt, and D. R. Garrod. 2007. Calcium-independent desmosomes of keratinocytes are hyper-adhesive. *J. Invest. Dermatol.* 127:775–781.
43. Mattey, D. L., and D. R. Garrod. 1986. Splitting and internalization of the desmosomes of cultured kidney epithelial cells by reduction in calcium concentration. *J. Cell Sci.* 85:113–124.
44. Cirillo, N., A. Lanza, and S. S. Prime. 2010. Induction of hyper-adhesion attenuates autoimmune-induced keratinocyte cell-cell detachment and processing of adhesion molecules via mechanisms that involve PKC. *Exp. Cell Res.* 316:580–592.
45. Zlatanova, J., S. M. Lindsay, and S. H. Leuba. 2000. Single molecule force spectroscopy in biology using the atomic force microscope. *Prog. Biophys. Mol. Biol.* 74:37–61.
46. Panorchan, P., M. S. Thompson, …, D. Wirtz. 2006. Single-molecule analysis of cadherin-mediated cell-cell adhesion. *J. Cell Sci.* 119:66–74.
47. Muller, D. J. 2008. AFM: a nanotool in membrane biology. *Biochemistry.* 47:7986–7998.
48. Bass-Zubek, A. E., L. M. Godsel, …, K. J. Green. 2009. Plakophilins: multifunctional scaffolds for adhesion and signaling. *Curr. Opin. Cell Biol.* 21:708–716.

49. Nekrasova, O., and K. J. Green. 2013. Desmosome assembly and dynamics. *Trends Cell Biol.* 23:537–546.

50. Waschke, J., C. Menendez-Castro, …, W. Baumgartner. 2007. Imaging and force spectroscopy on desmoglein 1 using atomic force microscopy reveal multivalent Ca(2+)-dependent, low-affinity trans-interaction. *J. Membr. Biol.* 216:83–92.

51. Rakshit, S., Y. Zhang, …, S. Sivasankar. 2012. Ideal, catch, and slip bonds in cadherin adhesion. *Proc. Natl. Acad. Sci. USA.* 109:18815–18820.

52. Baumgartner, W., N. Golenhofen, …, D. Drenckhahn. 2003. Ca2+ dependency of N-cadherin function probed by laser tweezer and atomic force microscopy. *J. Neurosci.* 23:11008–11014.

53. Rakshit, S., and S. Sivasankar. 2014. Biomechanics of cell adhesion: how force regulates the lifetime of adhesive bonds at the single molecule level. *Phys. Chem. Chem. Phys.* 16:2211–2223.

54. Tucker, D. K., S. N. Stahley, and A. P. Kowalczyk. 2014. Plakophilin-1 protects keratinocytes from pemphigus vulgaris IgG by forming calcium-independent desmosomes. *J. Invest. Dermatol.* 134:1033–1043.

55. Johnson, J. L., N. A. Najor, and K. J. Green. 2014. Desmosomes: regulators of cellular signaling and adhesion in epidermal health and disease. *Cold Spring Harb. Perspect. Med.* 4:a015297.

Biophysical Journal, Volume *119*

Supplemental Information

Desmosomal Hyperadhesion Is Accompanied with Enhanced Binding Strength of Desmoglein 3 Molecules

Michael Fuchs, Anna Magdalena Sigmund, Jens Waschke, and Franziska Vielmuth

Results

Cells lacking Pkp1 or 3 have reduced levels of Dsg3 after EGTA treatment

We investigated the expression and distribution of Dsg3 and actin using immunostainings. Interestingly, in wt murine keratinocytes Dsg3 and actin staining showed gaps (indicated by white arrows) when cells were treated with EGTA after 24 h in high Ca^{2+}-medium. After 72 h in high Ca^{2+} we found that Dsg3 and actin are properly located at the cell membrane and observed no gaps even after EGTA treatment in wt. However, Dsg3 staining was slightly reduced (Figure S1A). In contrast, Pkp1-deficient cells revealed a drastic phenotype with gaps after EGTA treatment at 24 h and 72 h of differentiation with reduced levels of Dsg3 at the cell membranes (Figure S1B) resembling the results from dissociation assays. Pkp3-deficient cells showed no reduced intensity of Dsg3 at the cell membrane after EGTA treatment at both time points (Figure S1C) but a more blurred distribution along the cell membrane. This is in line with their diminished ability to acquire hyper-adhesion in dissociation assays. The results suggest that Pkp1 and 3 both are important for hyper-adhesion in murine keratinocytes by contributing to a proper localization of Dsg3.

Materials and Methods

Tissue culture and human *ex-vivo* hyper-adhesion model

A small piece of skin from the shoulder area, < 24 h post mortem, was taken from each body donor and cut into equal pieces (1 cm × 1 cm). The age of the body donors ranged from 74 to 95 years. The samples were incubated in Dulbecco modified Eagle medium (DMEM) with 5 mM of ethylene glycol tetraacetic acid (EGTA) for 1.5 h or 24 h respectively at 37°C and 5% CO_2. Skin samples were afterwards embedded in TissueTec (Leica Biosystems, Nussloch,

Germany) and cut into 7 µm thick slices using a cryostat microtome (CryoStar^{TM} NX70, Thermo Scientific^{TM}, Waltham, Massachusetts, USA).

Cell culture

Wild type (wt) and Pkp1- or 3- (Pkp k.o.) deficient murine keratinocytes (MKZ) were isolated and immortalized as described before (kindly provided by Prof. Dr. Hatzfeld, University of Halle (Saale)) [1, 2]. A stable Dsg3 k.o. cell line of mouse epidermal keratinocytes (MKZ) was generated by spontaneous immortalization from Dsg3$^{-/-}$ and $^{+/+}$ C57BL/6J mice. Epidermis was gained from neonatal mice by overnight incubation of the skin with dispase II (Sigma-Aldrich, Munich, Germany). Epidermal cells were physically washed out after treatment for 1 h with accutase (Sigma-Aldrich, Munich, Germany) and seeded in Dulbecco's modified Eagle's medium (DMEM) (Life Technologies; Carlsbad; CA; USA) supplemented with 10 % Chelex-treated fetal calf serum (Biochrom, Berlin, Germany), 50 units/ml penicillin (AppliChem, Darmstadt, Germany), 50 µg/ml streptomycin (AppliChem), 1 mM sodium pyruvate, 0.18 mM adenine, 0.5 µg/ml hydrocortison, 5 µg/ml insulin, 100 pM cholera toxin (all 5 from Sigma-Aldrich, Munich, Germany), 10 ng/ml epidermal growth factor (Life Technologies; Carlsbad; CA; USA) and 2 mM GlutaMAX (Life Technologies; Carlsbad; CA; USA) on collagen I (rat tail; BD Bioscience, New Jersey, US) coated T25 culture flasks and maintained at 35°C and 5 % CO_2. After passaging for 10-15 times keratinocytes immortalized spontaneously while other epidermal cells died. For all experiments with MKZ, cells were switch to high Ca^{2+} (1.2 mM) containing medium after reaching confluency and grown for 24 h or 72 h, respectively, before experiments were conducted.

Immunostaining

Immunofluorescence of skin sections was done as described elsewhere [3]. Briefly summarized, skin sections were fixed with 4% formaldehyde, permeabilized with 1% Triton

X-100 and incubated with primary antibodies. For human skin samples two different primary antibodies were used (Table S1).. As secondary antibodies Cy-labelled goat-anti-mouse and –rabbit secondary antibodies (Dianova, Hamburg, Germany) were used, respectively. Further DAPI (Roche, Mannheim, Germany) was used to visualize the cells nuclei. Quantification was done with ImageJ Software using the selection brush tool. The raw integrated density was measured along all cell membranes and then divided by the measured area. Murine keratinocytes were fixed, 24 h or 72 h after Ca^{2+} switch respectively, in pure ethanol for 30 min on ice followed by three min aceton at room temperature. Primary antibodies were Desmoglein 3 pAb (Biozol Diagnostica, Eching, Germany), Alexa 488-phalloidin (Dianova, Hamburg, Germany) and DAPI. Images were taken with a Leica SP5 confocal microscope using a 63x NA 1.4 PL APO objective controlled by LAS AF software (Leica, Mannheim, Germany).

Antibody against:	In Figure 4, S3 and S4	Figure S4
Dsg1	Desmoglein 1-P124 mAb (Progen Biotechnik GmbH, Heidelberg, Germany)	A9812 pAb (Abclonal Technology, USA)
Dsg3	Desmoglein 3 pAb, E-AB-62720 (Biomol GmbH, Hamburg, Germany)	5G11 mAb (Invitrogen, USA)
Dsc1	Desmocollin 1 pAb (1), abx176152 (Abbexa, Cambridge, United Kingdom)	L15, sc-18115, pAb (2), (Santa Cruz, Dallas, TX, USA)
Dsc3	Desmocollin 3 mAb (Progen Biotechnik GmbH, Heidelberg, Germany)	Abx334157 pAb, (Abbexa, Cambridge, United Kingdom)

Table S1: Used primary antibodies for human skin samples.

Crosslinking, Electrophoresis and Western blot analysis

After washing with PBS cells were lysed with SDS-lysis buffer (25 mmol/l HEPES, 25 mmol/l NaF and 1% SDS, pH 7.4) followed by sonication on ice. The amount of protein was determined with the Pierce™ BCA Protein Assay Kit (Thermo Fisher, USA). Western blotting was implemented following established protocols [4].

The membrane-impermeable cross-linker ethylene glycolbis (sulfosuccinimidylsuccinate) (Sulfo-EGS) (Pierce Biotechnology, Rockford, USA) was used for detection of oligomerization of desmosomal cadherins. The experimental approach followed a well-established protocol [5, 6]. In brief, cells were subjected to respective experimental conditions, washed three times with cold PBS and Sulfo-EGS was added to the cells at a concentration of 2 mM for 30 min at room temperature. In order to stop the reaction, TBS was added at a concentration of 50 mM and incubated for 15 min. Western blotting to detect crosslinked proteins was performed following a standard protocol. For quantification, the raw integrated density of the oligomer band was first divided by the band of oligomer plus monomer. Afterwards the EGTA-treated column was divided by the non-EGTA treated column to obtain the oligomerization ratio.

Data processing and Statistics

For image processing Photoline software (Computerinsel, Bad Gögging, Germany) was applied. AFM images and data analysis of measured force-distance curves were processed with JPK data processing software (Bruker Nano GmbH, Berlin, Germany). Further AFM parameters were determined with Origin Pro 2016, 93G (Northampton, MA, USA). For densitometric measurements ImageJ software (NIH, Bethesda, USA) was used. Other data shown in this study were evaluated and depicted with Excel (Microsoft, Redmond, WA, USA).

For statistical significance in case of two groups we applied two-tailed Student´s t test. For multiple groups analysis of variance (one-way ANOVA) followed by Bonferroni post hoc test was done. Error bars are standard error of the mean or standard deviation as indicated. Significance was assumed at a p-value < 0.05.

Supporting References

1. Keil, R., K. Rietscher, and M. Hatzfeld, *Antagonistic Regulation of Intercellular Cohesion by Plakophilins 1 and 3.* Journal of Investigative Dermatology, 2016. **136**: p. 8.
2. Rietscher, K., A. Wolf, G. Hause, A. Rother, R. Keil, T.M. Magin, M. Glass, C.M. Niessen, and M. Hatzfeld, *Growth Retardation, Loss of Desmosomal Adhesion, and Impaired Tight Junction Function Identify a Unique Role of Plakophilin 1 In Vivo.* Journal of Investigative Dermatology, 2016. **136**(7): p. 8.
3. Egu, D.T., E. Walter, V. Spindler, and J. Waschke, *Inhibition of p38MAPK signalling prevents epidermal blistering and alterations of desmosome structure induced by pemphigus autoantibodies in human epidermis.* British Journal of Dermatology, 2017. **177**(6).
4. Hartlieb, E., B. Kempf, M. Partilla, B. Vigh, V. Spindler, and J. Waschke, *Desmoglein 2 Is Less Important than Desmoglein 3 for Keratinocyte Cohesion.* PLoS ONE, 2013. **8**(1): p. 12.
5. Nie, Z., A. Merritt, M. Rouhi-Parkouhi, L. Tabernero, and D. Garrod, *Membrane-impermeable Cross-linking Provides Evidence for Homophilic, Isoform-specific Binding of Desmosomal Cadherins in Epithelial Cells.* JOURNAL OF BIOLOGICAL CHEMISTRY, 2011. **286**(3): p. 11.
6. Fuchs, M., M. Foresti, M.Y. Radeva, D. Kugelmann, R. Keil, M. Hatzfeld, V. Spindler, J. Waschke, and F. Vielmuth, *Plakophilin 1 but not plakophilin 3 regulates desmoglein clustering.* Cellular and Molecular Life Sciences, 2019.

Figures:

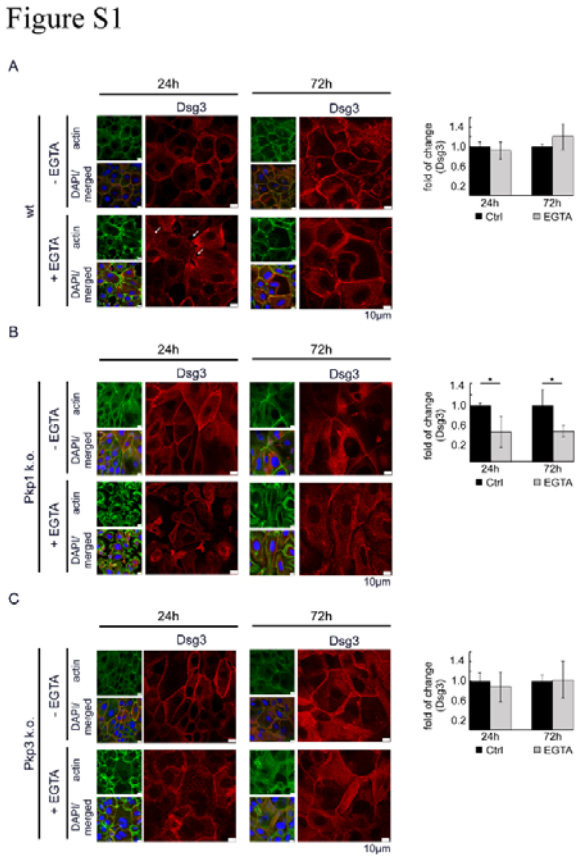

Figure S1: Reduced levels of Dsg3 after EGTA treatment for Pkp1 or 3 lacking cells.

A/**B**/**C**: Murine keratinocytes were maintained for 24 h or 72 h in high Ca^{2+} medium and were subsequently subjected to Ca^{2+} chelation with EGTA for 90 min. Immunostaining for Dsg3 and actin revealed disturbed membrane localization after 24 h in high Ca^{2+} medium as well as gap formation between the cells (white arrows). In contrast, membrane staining was preserved after Ca^{2+} chelation in wt and Pkp3-deficient but not in Pkp1-deficient keratinocytes after 72h in high Ca^{2+} medium. DAPI was used to stain cell nuclei. Pictures show representatives of $n \geq 3$. Scale bar = 10 µm. *$p<0.05$ vs. corresponding control, error bars represent standard deviation.

Figure S2

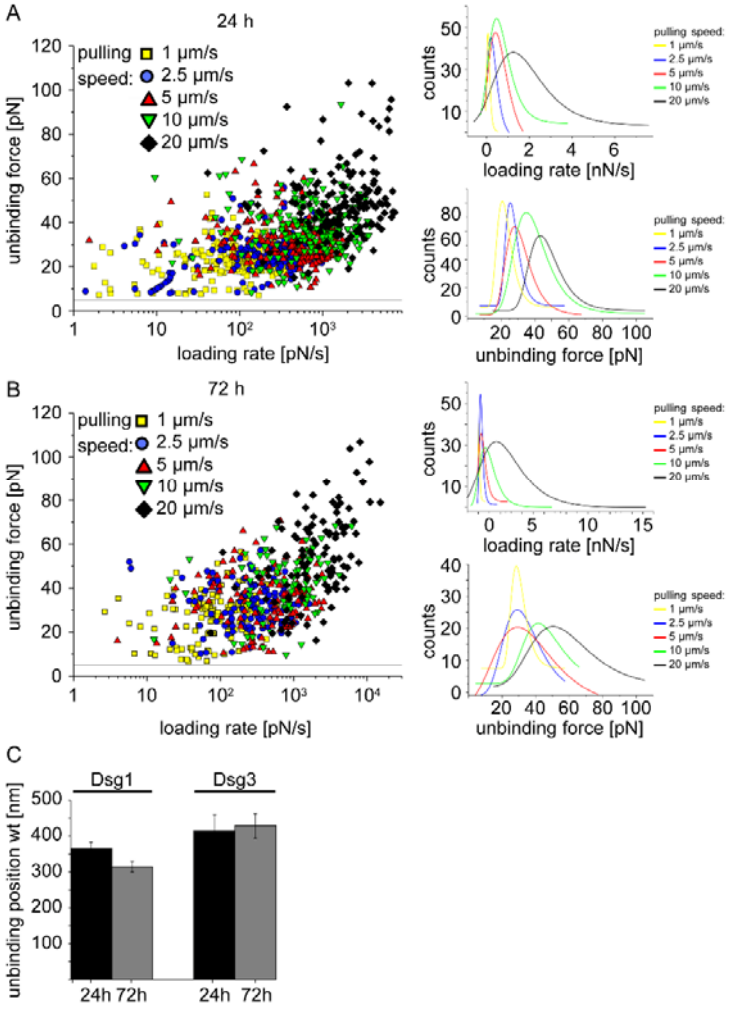

Figure S2: A-B: UF plotted against logarithmic loading rate with respect to their pulling speed after 24 h and 72h in high Ca2+ medium, shows an increase of UF and loading rate for higher pulling forces. Grey line indicates 5 pN threshold level, values below that line were excluded from analysis. On the right side the distribution of the loading rates and unbinding forces of the increasing pulling speeds is shown. n=8 with 2 cell borders/experiment. **C:** Unbinding position of Dsg1 and 3 coated tips comparing 24 h and 72 h in high Ca2+ medium shows no significant alterations. For Dsg1 n=4 and for Dsg3 n=6 were used for analysis, error bars represent error of the mean.

Figure S3

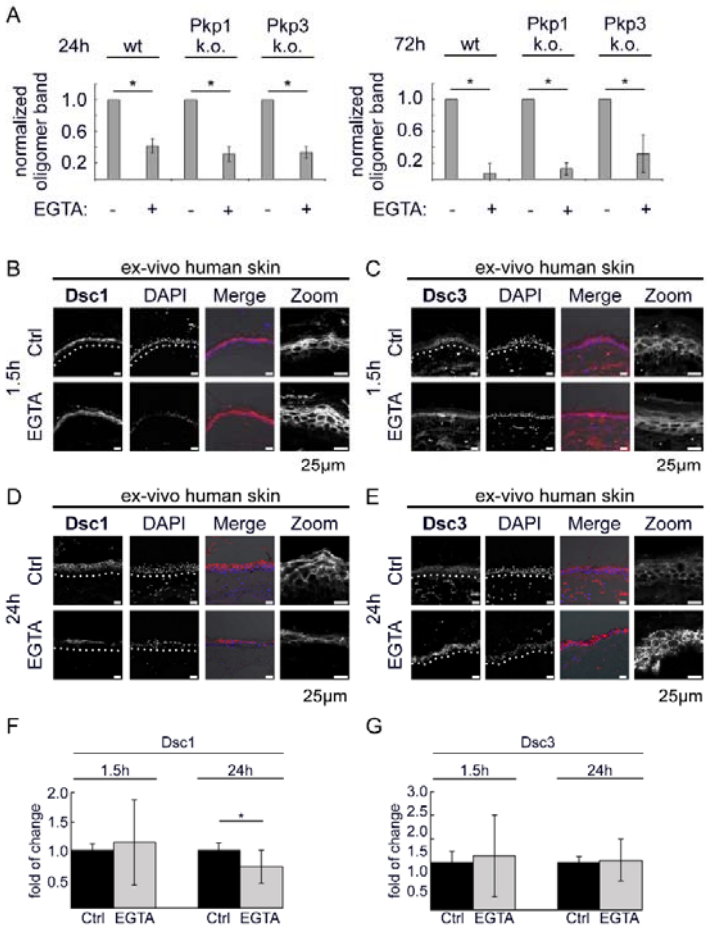

Figure S3: A: Quantification of oligomer band density of ECad shows significant decrease after EGTA treatment for all cell lines after 24h and 72h in high Ca^{2+} medium. n≥4, *p<0.05 vs. corresponding control, error bars represent standard deviation. B-**G:** Immunostaining for Dsc1 and 3 of human epidermis after 1.5h or 24h of EGTA incubation reveals reduced and fragmentated levels of Dsc1 but not Dsc3 staining. n≥3, *p<0.05 vs respective control, error bars represent standard deviation.

Figure S4

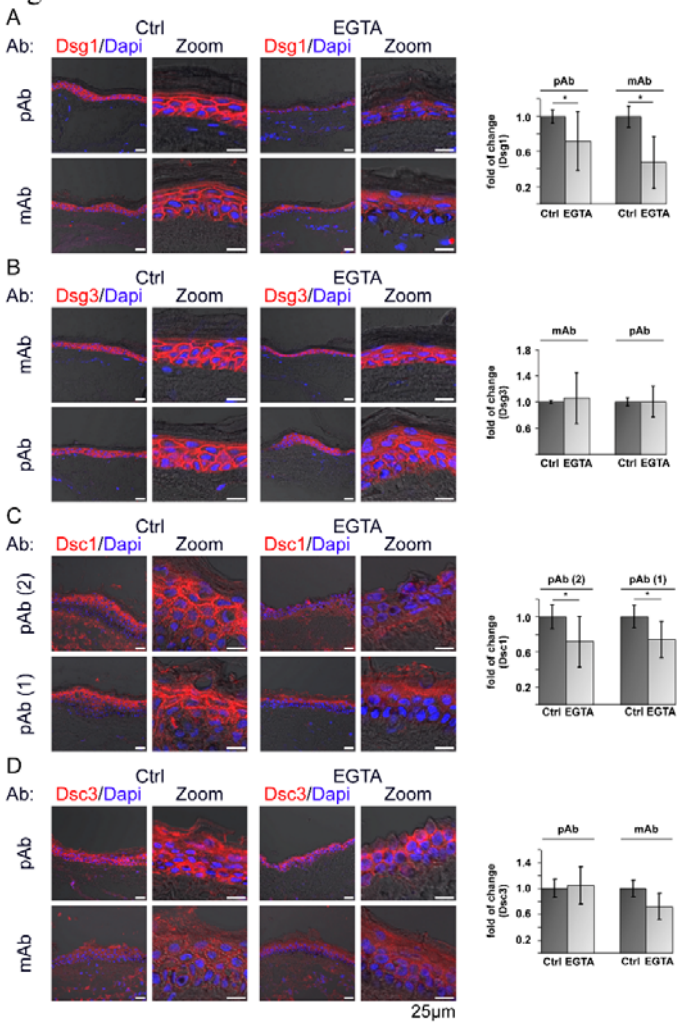

Figure S4: Immunostaining of respective desmosomal cadherins in human epidermis after 24h of EGTA treatment using two sets of primary antibodies. **A:** For Dsg1 both antibodies show a significant reduced membrane staining and protein amount after 24h EGTA treatment. **B:** Dsg3 immunostaining with two different primary antibodies show little alterations after 24h EGTA incubation. **C:** Significantly reduced membrane staining of Dsc1 after EGTA treatment is shown for both primary antibodies. **D:** For Dsc3 staining no difference can be found for the used primary antibodies. **A-D:** n=4, *p<0.05 vs corresponding control, error bars represent standard deviation.